Mesomorphic and Dielectric Properties of Heterocyclic Liquid Crystals with Different Terminal Groups

Juman A. Naser
Dept. of Chemistry/ College of Education for Pure Science (Ibn Al-Haitham)/ University of Baghdad
Received in:22/February/2016,Acceped in:30/March/2016

Abstract

A new hetrocyclic liquid crystal compounds containing 1,3,4-oxadiazole with different substituted in para position (Bromo, Chloro, Nitro and Methyl) were synthesized and characterized by melting points, FTIR Spectroscopy and ^{1}HNMR spectroscopy for [Cl-SR_6] and [NO_2-SR_6] compounds. The liquid crystalline properties of the synthesized compounds were studied by using hot-stage polarizing optical microscopy (POM), so they determined the transition enthalpies and entropies by using differential scanning calorimetery (DSC). All of the compounds show mesomorphic properties. The compounds [Br-SR_6], [Cl-SR_6] and [NO_2-SR_6] exhibit an enantiotropic dimorphism smectic (Sm) phase, while the compounds [Me-SR_6] showed nematic (N) phase throw cooling only. Continuously, permittivity dielectric properties, electrical conductivity, relaxation times and activation energies have been studied in the range of temperatures (70-150)°C at two frequencies (500) Hz and (1000) Hz. Generally, the results show the dielectric permittivity and relaxation time values increasing when raising temperature, while electrical conductivity values decrease with increasing temperature. The activation energy values were determined in terms of the Arrhenius plot.

Keywords: Heterocyclic, Schiff Bases, Nematic, Smectic, Liquid crystals, Dielectric permittivity, Electrical conductivity, Relaxation time, Activation energy.

Introduction

Liquid crystals are states of matter whose intermediate between crystalline solids and isotropic liquids [1-4]. Thermotropic liquid crystals can be classified into three different types, nematic, smectic and cholesteric according to the degree of order in their molecular structure [1]. They have been extensively investigated as a result to their large scale of applications in technology and industry [5,6]. Generally the extensive uses of liquid crystals in different fields depend on a various of their properties such as dielectric permittivity, dielectric anisotropy, order parameter, elastic constants and optical transmittance [7]. They are easily oriented and reoriented by electric or magnetic applied fields, Therefore the importance of dielectric properties lies in understanding the molecular structure of matter [8]. It is known that dielectric studies of liquid crystal substances are a valuable source of information about phase transition, molecular arrangement, molecular dynamics and specific intermolecular interactions, in both mesomorphic and isotropic phases [9,10].

The aim of the present paper is to prepare and identify liquid crystalline behavior of thermotropic liquid crystalline compounds, then study dielectric permittivity properties, electrical conductivity, relaxation time and activation energy at different temperatures.

Experimental

Chemical Materials

Most of chemical materials used were supplied from Aldrich-Sigma chemical company were used without further purification: absolute ethanol, para-bromo benzaldehyde, para-chloro benzaldehyde para-nitro benzaldehyde, para-methyl benzaldehyde, glacial acetic acid and ethanol 95%.

Instrumentation

FTIR spectra were recorded on an instrument model Shimadzu-8300 spectrophotometer by using potassium bromide disc. ^{1}H-NMR spectra were obtained with a varian mercury plus spectrometer 400 MHz instrument using DMSO solvent and TMS as internal standard. Uncorrected melting points were recorded on hot stage Gallen Kamp melting point apparatus. The optical behavior observations were made using Olympus BX40 microscope equipped with a Leitz Labrix12 pols hot stage and PR 660 controller. The textures shown by the compounds were observed using polarized light with crossed polarizers with the sample in a thin film sandwiched between a glass slide and cover slip. Differential scanning calorimetry (DSC) measurements were conducted with LINEEIS instruments DSC, Ramp rate: 5 degree centigrade per minute under nitrogen atmosphere. Temperature and heat flow calibrated with standard indium of purity >99.99%.

The dielectric behavior of the liquid crystals materials has been recorded by using LCR meter model hp-4274A multi frequency that based a hot stage polarizing microscope (POM) as described by Gray [11] The dielectric values were measured with range of temperatures (70-150)°C at two frequencies 500 Hz and 1000 Hz. The electrodes were two similar cells having active area of 1 cm^2 were prepared by using flat glass coated with indium tin oxide ITO. In this study, the sandwich cells were filled with samples through capillary action method. The thickness of cell was fitted by mylar spacer of (12 μm). The sample was heated to isotropic phase, then held until to attain thermal equilibrium, the data were recorded during cooling process each 5°C.

Synthesis of Compounds

The new compounds were synthesized according to Scheme 1.

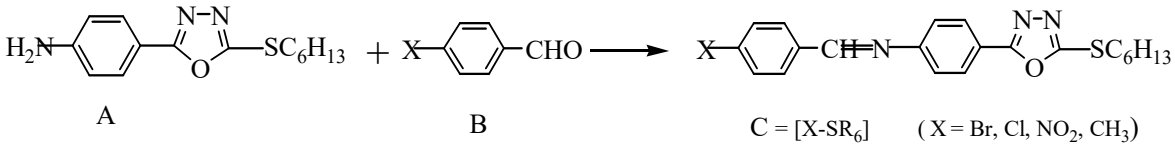

Scheme (1)

Synthesis of 1-(para-substituted benzylidene amino)-4-(2-n-hexylthio-1,3,4-oxadiazole-5yl) benzene [X-SR$_6$]

These model compound were prepared by dissolved (0.5 g, 0.002 mol) of 2-n-hexyl thio-5-(4-aminophenyl)-1,3,4-oxadizole were synthesized and published in previous work [12], in (10 mL) absolute ethanol then added para-substituted benzaldehyde (0.002 mol) and glacial acetic acid (3 drops). The mixture refluxed for 3 h, the solvent was evaporated and the residue crystallized from ethanol 95%, then yellow products have been collected.

Results and Discussion

The four compounds [Br-SR$_6$], [Cl-SR$_6$], [NO$_2$-SR$_6$] and [Me-SR$_6$] were synthesized according to Scheme 1. The FTIR spectroscopy for all synthesized compounds and ^{1}HNMR spectroscopy of compounds [Cl-SR$_6$] and [NO$_2$-SR$_6$] confirmed and indicated the structure of respective compounds. The thermodynamic data of transitions phase for all synthesized compounds are listed in Table 1.

Characterization of Compounds

4-(4′-X-benzylideneamino)-4-(2-n-hexyl-thio-1,3,4-oxadiazole-5-yl) benzene [X-SR$_6$]

Figures (1), (2), (3) and (4) showed the FT-IR spectra for all compounds [X-SR$_6$] showed the disappearance of absorption band of ν NH_2 in the range (3221-3414) cm^{-1} and carbonyl group for aldehyde at (1700) cm^{-1}, and the appearance of absorption band at (1593-1606) cm^{-1} attributed to ν C=N stretching and another band at (835-850) cm^{-1} which attributed to bending out of plane of hydrogen atoms of benzene ring that substituted in para position, all that indicated the structure of Schiff bases.

^{1}HNMR spectrum of compounds [Br-SR$_6$] and [Cl-SR$_6$] Figures (5) and (6) respectively, showed the following characteristic chemical shift signals by using a DMSO as a solvent: A triplet signals at δ (0.8-1.9) ppm attributed to three protons of terminal for CH_3 aliphatic group. Eight protons multiplet at δ (2.4-2.7) ppm that could be due to (–CH_2CH_2 –) protons. A triplet signals at δ (3.2-3.5) ppm attributed to two protons of SCH_2. Eight aromatic protons of (AB) doublets appear as two doublets signals at δ (7.3- 8.5) ppm due to central benzene rings. Singlet signal at δ (8.8-9.0) ppm which attributed to one proton of azomethine group CH=N.

Mesomorphic Properties of Compounds

The mesophases textures of all compounds were determined from textural observation by thermal microscopy under an optical polarizing microscope during heating and cooling cycles. Phase transition temperatures that observed by POM have been found to be in agreement with the corresponding differential scanning calorimetry (DSC).

It is well known that the different substituted groups influence in the polarizability and the geometry of the molecules that determined the type and phase transition temperatures of the mesophases. In this work a new 1,3,4-Oxadizole unit with different terminal groups

derivatives were synthesized and their liquid crystalline properties were studied. All synthesized compounds examined by differential scanning calorimeter (DSC) and verified by using hot-stage polarized optical microscopy (POM). Phase transition temperatures on heating from crystal phase (Cr) to liquid crystalline phases (LC) then the transition to isotropic liquid (I) and on cooling from isotropic liquid (I) to liquid crystalline phases (LC) then crystal phase (Cr). The mesophase type (texture identity) was investigated using POM. In addition, the thermodynamic data (enthalpies and entropies) of these compounds were determined by using DSC.

Figures (7), (8), (9) and (10) show thermograms of all synthesized compounds of series [X-SR_6]. The phase transitions and corresponding thermodynamic changes data for all compounds were determined by DSC and summarized in Table 1. All these compounds exhibited mesomorphic behavior. [Br-SR_6], [Cl-SR_6] and [NO_2-SR_6] displayed enantiotropic smectic Sm phases, while [Me-SR_6] has been appeared enantiotropic nematic N phase.

This behaviour of above could be explained in term of terminal /lateral (t/l) interaction forces ratio. When this ratio is high, compounds tend to give less ordered mesophases (nematic mesophase) as compound [Me-SR_6]. While this ratio is low that means the terminal group is now sufficiently bulky and thus more polarizable to overcome residual terminal cohesive forces.

The DSC thermogram of compound [Br-SR_6] shows three endothermic transitions the first one at 101°C which attributed to crystal-crystal (Cr-Cr) transition, the second at 107.3°C attributed to crystal smectic transition, while transition to isotropic phase appeared at 139.5°C, Figure (7).

The DSC thermogram of the thermal behavior of compound [Cl-SR_6] was shown in Figure (8), which exhibited a peak at 105.6°C that represented an actual transition temperature from crystal to smectic phase, while transition to isotropic appeared at 135.8°C.

Continuously, the DSC thermogram of compound [NO_2-SR_6] displays two endothermic transitions, the first one appears at 141.8°C and the second appears at 156.9°C that attributed to crystal smectic transition and transition to smectic isotropic phase respectively, Figure (9). While the DSC thermogram of compound [Me-SR_6] did not show any endothermic mesogenic transition but appeared exothermic nematic transitions at 104.4°C, Figure (10).

Compounds [Br-SR_6], [Cl-SR_6] and [NO_2-SR_6] showed the presence of a smectic A (Sm_A) phase, while [Me-SR_6] seemed Nematic (N) phase, all transitions were observed on both heating and cooling cycles. Figure (11a,b) shows typical focal conic Sm_A texture of [Br-SR_6]. So Figure (12a,b) appeared focal conic Sm_A texture of [Cl-SR_6]. High order Sm_E phase of compound [NO_2-SR_6] was determined by the formation of the domain mosaic texture as shown in Figure (13a,b). On further cooling from the isotropic liquid, Figure (14a,b) showed N phase of compound [Me-SR_6] which presented characteristic a droplet and a marble texture.

Dielectric Properties

Dielectric Permittivity Properties

The real dielectric parameters (έ) of the prepared liquid crystal materials were calculated from the ratio of the capacitance of the material to the capacitance of the same electrode system with vacuum, using the following equations (1) and (2) given by [13,14]:

$$\acute{\varepsilon} = C_x/C_a \quad \ldots\ldots\ldots (1)$$

where (C_x) the capacitance of sample and (C_a) the capacitance without sample of free space which calculated from formula:

$$C_a = (0.0885)A/t \ldots\ldots\ldots (2)$$

where A is area of the cell in m^2 which is equal to (0.001) m^2 and t is the thickness of the sample in sandwich cell which is equal to (12) μm. Figure (15) shows the variation of real dielectric permittivity with a range of temperatures for these materials at frequency (500) Hz and (1000) Hz.

The Figure (15) shows that the dielectric permittivity values (έ) decrease as frequency increases. This is due to the effect of dipole moment of liquid crystal molecules is aligned along applied electrical field. The decrease in permittivity with frequency can be explained on the basis of Koop's theory [15].

Generally, The dielectric permittivity values have been increased gradually with increases temperature, that is due to increasing in thermal motion of molecules.

Continuously, the dielectric permittivity varieties from one liquid crystal to another one depending on atomic polarization and electronic polarization in molecule [14].

The loss angle (tan δ) values were calculated using the equation (3) [14,16]:

$$tan\delta = 1/\omega . R . C_x \dots\dots\dots\dots (3)$$

where $\omega\ is\ (2\pi f)$ and f is the applied frequency, R is the resistance of the materials and C_x is the capacitance of the material in pF unit.

The imaginary dielectric permittivity ($\acute{\varepsilon}$) or dielectric loss was determined from equation (4) [7, 16]:

$$\acute{\varepsilon} = tan\delta . \acute{\varepsilon} \dots\dots\dots\dots (4)$$

Figure (16) shows the temperature dependence of imaginary dielectric permittivity for this liquid crystal materials at frequency 500 Hz and 1000 Hz.

The dielectric loss values ($\acute{\varepsilon}$) decrease with increasing temperature, this is attributed to the increasing in thermal energy of molecules which lead to decrease in lost energy along applied external field.

In comparison between the imaginary dielectric permittivity values at two applied frequencies, these have lower values at 1000 Hz than that at 500 Hz as result to inability the molecules are consisting of the alternating in electrical field at higher frequency.

Electrical Conductivity Properties

The electrical conductivity values have been determined for that prepared liquid crystals in the same temperature range (70-150)°C for both frequencies 500 Hz and 1000 Hz from equation (5) [17].

$$\sigma_{AC} = \varepsilon_0 \acute{\varepsilon}\, \omega \dots\dots\dots\dots (5)$$

where ε_0 is the free space of dielectric permittivity which is equal to ($8.85*10^{-12}$) F/m, $\acute{\varepsilon}$ is imaginary dielectric permittivity and $\omega = 2\pi f$ is the cyclic frequency.

The Figure (17) shows variation of electrical conductivity values in this temperatures range and two frequencies.

The electrical conductivity values σ_{AC} decrease with temperature increasing. This is due to the increasing in the random mobility of charge carriers as a result to rising in temperatures.

Additionally, the thermal conductivity values at 1000 Hz are greater than that in 500 Hz, this attributed to the oscillation time of liquid crystal molecules is smaller than the relaxation time in the lowest frequency.

Relaxation Times

The following equation (6) was used to calculate the relaxation time values (τ) [18]:

$$\tau = 1/2\pi f.tan\delta \quad \dots\dots\dots\dots (6)$$

The Relaxation times of the samples with temperatures variation have been represented in Figure (18). The relaxation time values (τ) increase with increasing in temperature, as result to an increase in the period from one orientation state to another that separated by a potential barrier. The relaxation time has great importance in liquid crystal devices which depends on molecular alignment, the gap energy and many other parameters.

Activation Energies

The activation energy values (E_a) is determined by using an Arrhenius equation (7) [18-20]:

$$\tau = \tau_0 e^{-Ea/k_B T} \quad \dots\dots\dots\dots (7)$$

where τ_0 is the pre-exponential factor, k_B is Boltzmann's constant and T is the absolute temperature.

The values of activation energies have been given in Table (2), E_a values at 1000 Hz were larger than that in 500 Hz, as a result to the fast oscillation time of alternating field which did not give enough time for the molecules to follow theirs alternation in high frequency.

The Arrhenius equation describes the behavior for a process from initial orientation to the second orientation which described by potential barrier and the height of the barrier translates the activation energy, which plays a crucial role in large scale of applications, therefore it has been calculated by using Arrhenius plot.

References

1. Demus, D.; Goodby, J.; Gray, G. W.; Spiess, H. W. and Vill, V., (1998), "Handbook of Liquid Crystals", 1, Wiley-VCH, New York.
2. Rizvi, T. Z., (2003), "Liquid Crystalline Biopolymers: A New Arena for Liquid Crystal Research", Journal of Molecular Liquids, 106, (43-53).

3. Chong, T.T.; Heidelberg, T.; Hashim, R. and Gary, S., (2007), "Computer modelling and simulation of thermo tropic and lyotropic alkyl glycoside Bilayers", Liq.Cryst., 34, (267-281).
4. Yoshizawa, A.; Nakata, M. and Yamaguchi, A., (2006), "Phase transition behaviour of novel Y-shaped liquid crystal oligomers", Liq. Cryst., 33, (605-609).
5. Kato, T., (2002), "Self-Assembly of Phase-Segregated Liquid Crystal Structures", Science, 295 , (2414-2418).
6. Iannacchione, G.S. , (2004), "Review of liquid-crystal phase transitions with quenched random disorder", Fluid Phase Equlib., 177-187, (222- 223).
7. Taraka, N.; Rao, R.; Raju, R.; Sita, A. and Venkayya, P., (2014), "Thermodynamical, dielectric and optical properties of liquid crystal sample signalling SmA point", African Journal of physics, 2, (1-7).

8. Johri, M.; Saxena, A.; Johri, S.; Saxena, S. and Singh, D. P., (2011), "Dielectric relaxation studies in 5CB nematic liquid crystal at 9 GHz under the influence of external magnetic field using microwave cavity spectrometer", Pramana – J. Phys., 76, 4, (621-628).
9. Meier, G.; Sackmann, E. and Grabmaier, J. G., (1975), "Application of Liquid Crystals", Springer-Verlag: Berlin.
10. Kresse, H. In: Brown, G. H. (Ed.), (1983), "Advances in Liquid Crystals", Academic: New York.
11. Gray, G.W., (1962), "Molecular structure and the properties of liquid crystals", Academic Press: New York.
12. Naser, J. A.; Himdan, T. A. and Al-Dujaili, A. H., (2014), "Synthesis and characterization of Schiff-base liquid crystal containing 1,3,4-oxadizole", International academic research for multidisciplinary, 2, 2320, (415-426).
13. Chemie, V. F., (2009), "Liquid crystal systems for microwave applications", Dissertation, Technical University Darmstadt.
14. Houtepen, S. A. A., (2010), "Dielectric loss estimation using damped AC voltages", MSc. Thesis, Delft University of Technology.
15. Koops, C.G., (1951), "On the dispersion of resistivity and dielectric constant of some semiconductors at audio frequencies", Phys. Rev., 83, (121-124).
16. Javed, A.; Akram, M. and Shafiq, M. I., (2006), "Dielectric properties of cholesterol derivatives", Journ. Phys., 51, 7–8, (819–826).
17. Gornitska, O.P.; Kovalchuk, A.V.; Kovalchuk, T.N.; Kopcansky, P.; Timko, M.; Zavisova, V.; Koneracka, M.; Tomasovicova, N.; Jadzyn, J. and Studenyak, I. P., (2009), "Dielectric properties of nematic liquid crystals with Fe_3O_4 nanoparticles in direct magnetic field: semiconductor physics", Quantum Electronics & Optoelectronics, 12, 13, (309-314).
18. Blinov, L. M. and Chigrinov, V. G., (1994), "Electro optical effect in liquid crystal material", Springer-Verag, New York.
19- Tripathi, P.; Dixit, S. and Manohar R., (2013), "Effect of bridging group on the dielectric properties of liquid crystals", Chemical Rapid Communications, 1, 2, (50-55).
20. Malik, P.; Chaudhary, A.; Mehra, R. and Raina, K. K., (2012), "Electrooptic and dielectric studies in cadmium sulphide nanorods/ferroelectric liquid crystal mixtures", Advances in Condensed Matter Physics Article ID 853160, (1-8).

Table (1): Phase transition temperatures, transition enthalpies and transition entropies for liquid crystal compounds [X-SR_6] upon heating and cooling.

Compound	Temperature ^0C	Transitions	ΔH (J/mol)	ΔS (J/K. mol)
Br-SR_6	101	Cr→Cr	+4683.15	+12.521
	107	Cr→Sm	+13290.4	+34.974
	139.5	Sm→I	+5411.14	+14.372
	123.5	I→Sm	-2383.7	-6.019
	89.1	Sm→Cr	-14298.02	-39.486
Cl-SR_6	105.6	Cr→Sm	+25635.9	+67.712
	135.8	Sm→I	+4869.91	+11.913
	130.8	I→Sm	-2680.65	-6.638
	86.9	Sm→Cr	-15908.1	-44.201
NO_2-SR_6	141.8	Cr→Sm	+446.9	+1.077
	156.9	Sm→I	+29647.1	+68.963
	157.5	I→Sm	-446.9	-1.038
	133.1	Sm→Cr	-29909.5	-73.651
Me-SR_6	75.3	Cr→Cr	+213.76	+0.614
	108.3	Cr→I	+39830.1	+104.458
	104.4	I →Ne	-520.26	-1.378
	76.7	Ne→Cr	-33194.85	-94.924

Table (2): Activation energy values for liquid crystal compounds.

Compound	Ea (J/mol) (100 Hz)	Ea (J/mol)(1000 Hz)
Br-SR_6	2432.67	2798.49
Cl-SR_6	3205.05	5851.39
NO_2-SR_6	3404.58	4705.72
Me-SR_6	1849.86	2813.45

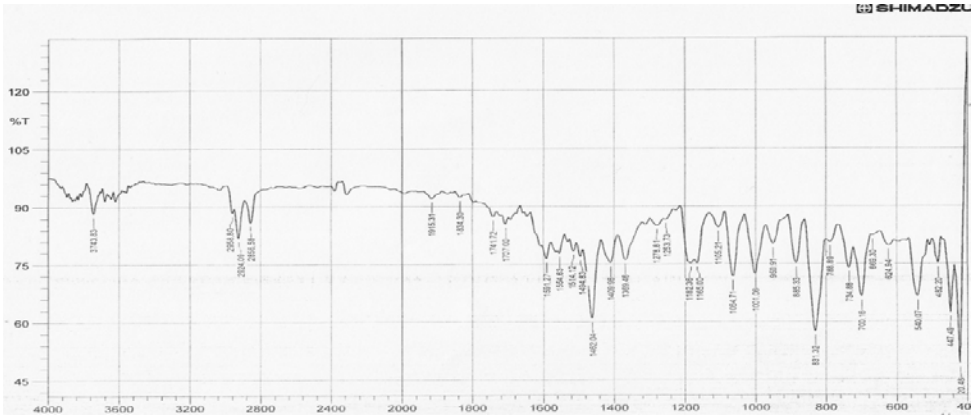

Figure (1): FT-IR spectrum of compound [Br-SR_6].

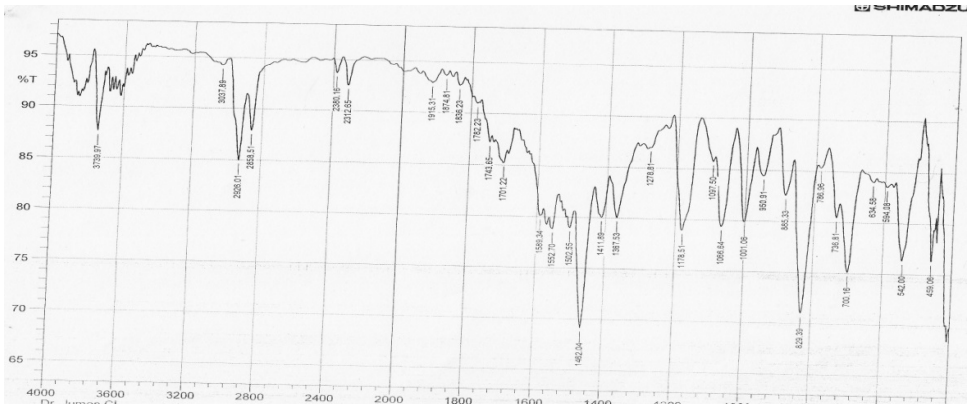

Figure (2): FT-IR spectrum of compound [Cl-SR_6].

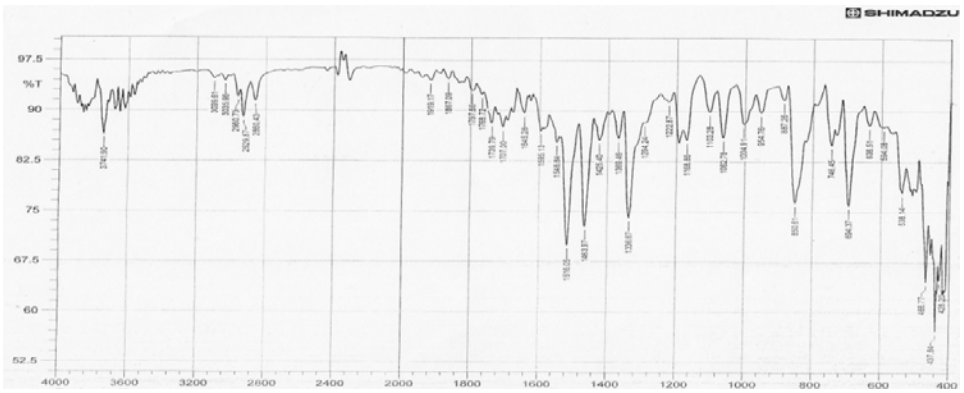

Figure (3): FT-IR spectrum of compound [NO_2-SR_6].

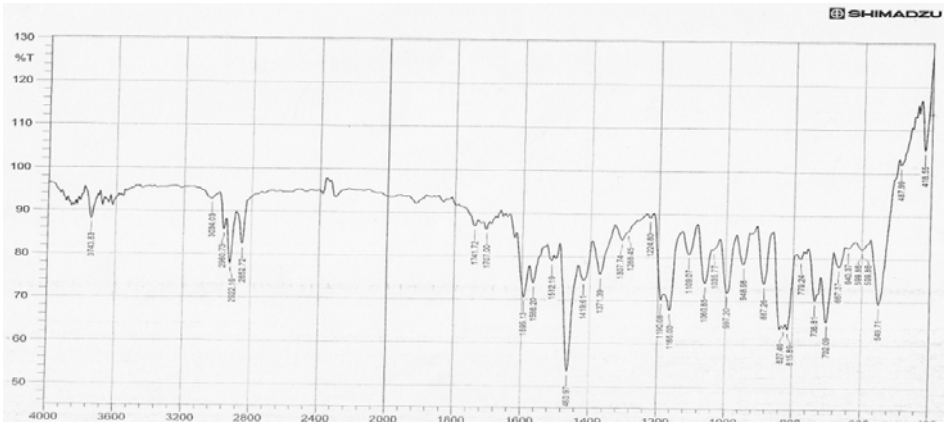

Figure (4): FT-IR spectrum of compound [Me-SR_6].

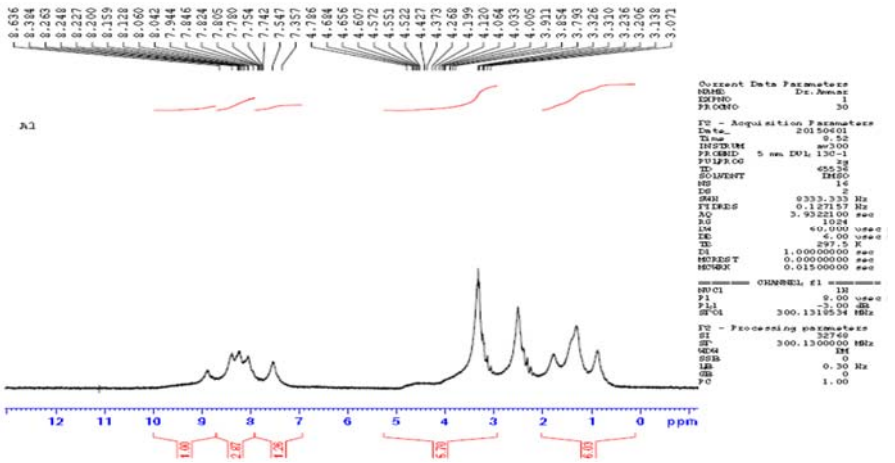

Figure (5):.^{1}H NMR spectrum of compound [NO_2-SR_6].

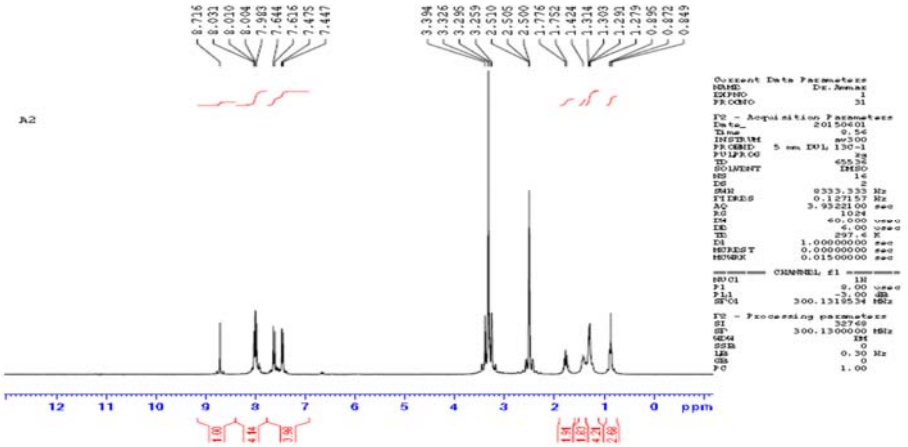

Figure (6):.^{1}H NMR spectrum of compound [Cl-SR_6].

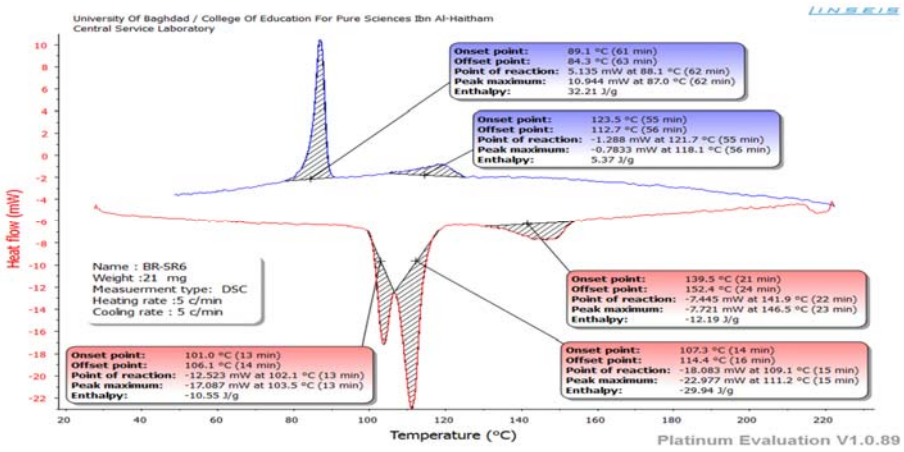

Figure (7): DSC Thermogram of compound [Br-SR_6] upon heating and cooling.

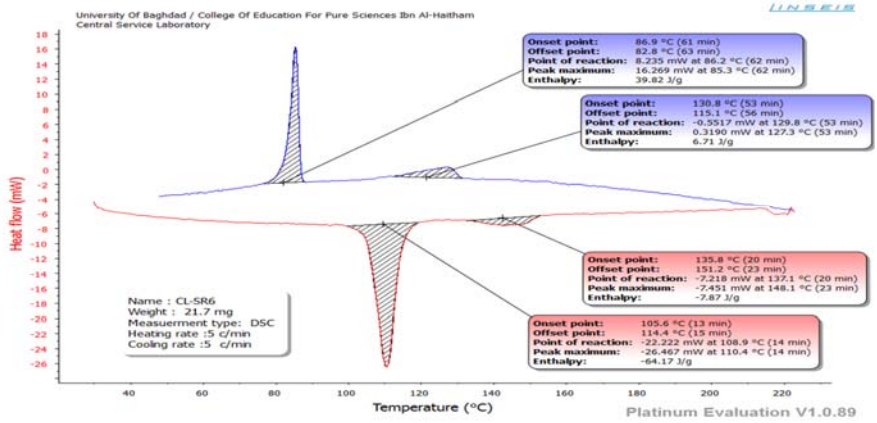

Figure (8): DSC Thermogram of compound [Cl-SR_6] upon heating and cooling.

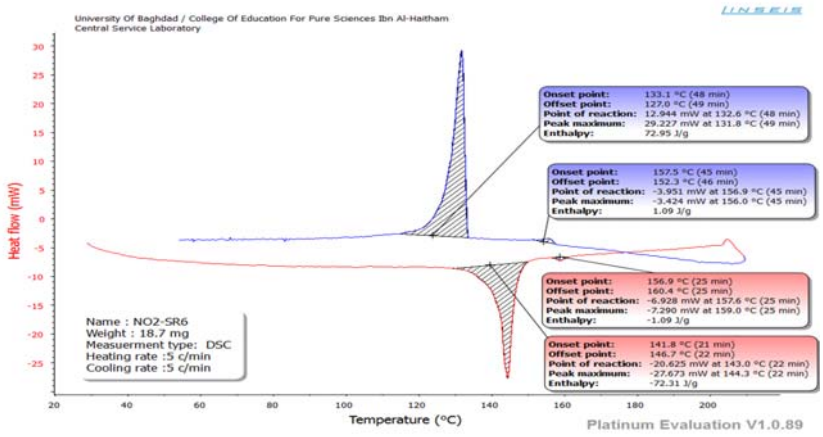

Figure (9): DSC Thermogram of compound [NO_2-SR_6] upon heating and cooling.

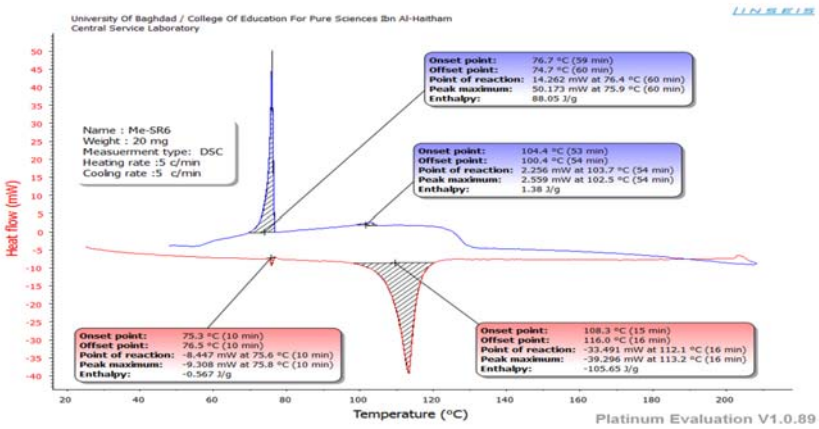

Figure (10): DSC Thermogram of compound [Me-SR_6] upon heating and cooling.

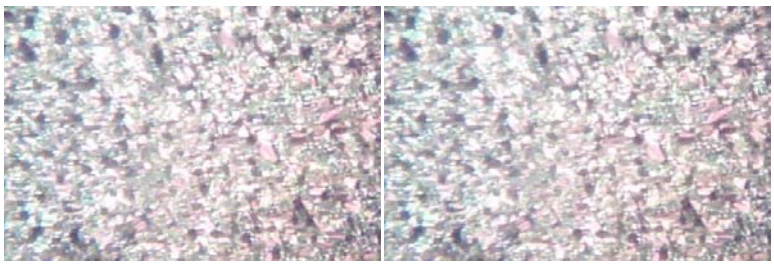

(a) **(b)**

Figure (11): Polarizing photomicrograph of Smectic phase Sm_A of compound [Br-SR_6] on cooling: (a) A focal conic Sm_A texture at 120 ºC; (b) A focal conic Sm_A texture at 110 ºC.

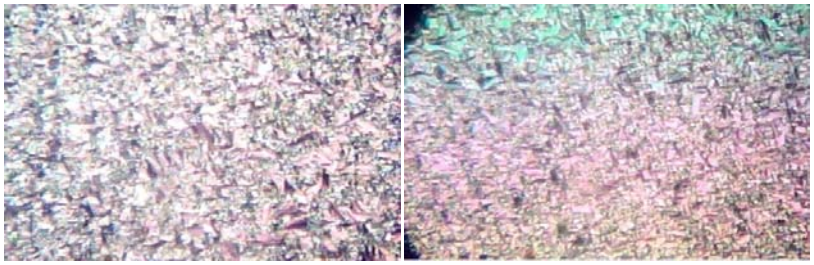

(a) **(b)**

Figure (12):Polarizing photomicrograph of Smectic phase Sm_A of compound [Cl-SR_6] on cooling: (a) A focal conic Sm_A texture at 125 ºC; (b) A focal conic Sm_A texture at 108 ºC.

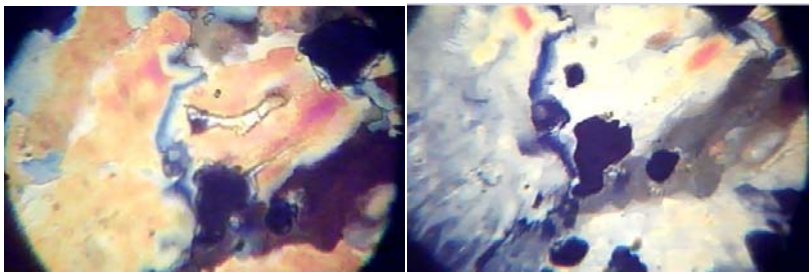

(a) (b)

Figure (13):Polarizing photomicrograph of Smectic phase Sm_E of compound [NO_2-SR_6] on cooling: (a) A mosaic Sm_E texture at 152 ºC; (b) A mosaic Sm_E texture at 143 ºC.

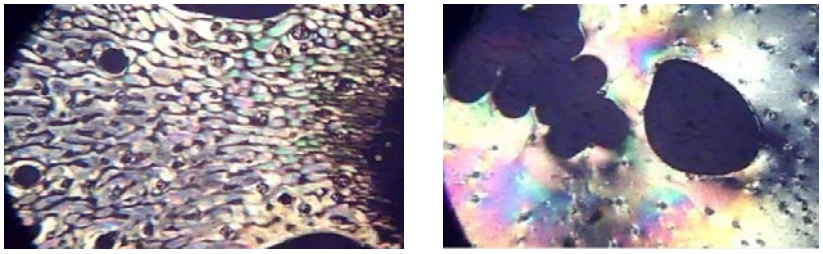

(a) (b)

Figure (14):Polarizing photomicrograph of Nematic phase N of compound [Me-SR_6] on cooling: (a) A droplet Nematic texture at 98 ºC; (b) A marble Nematic at 87 ºC.

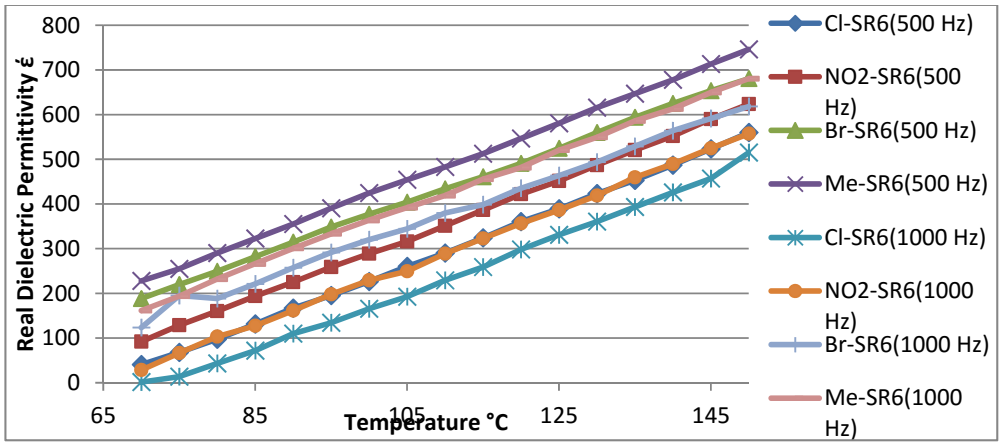

Figure (15): Temperature dependence of real dielectric permittivity at (500 and 1000) Hz for samples.

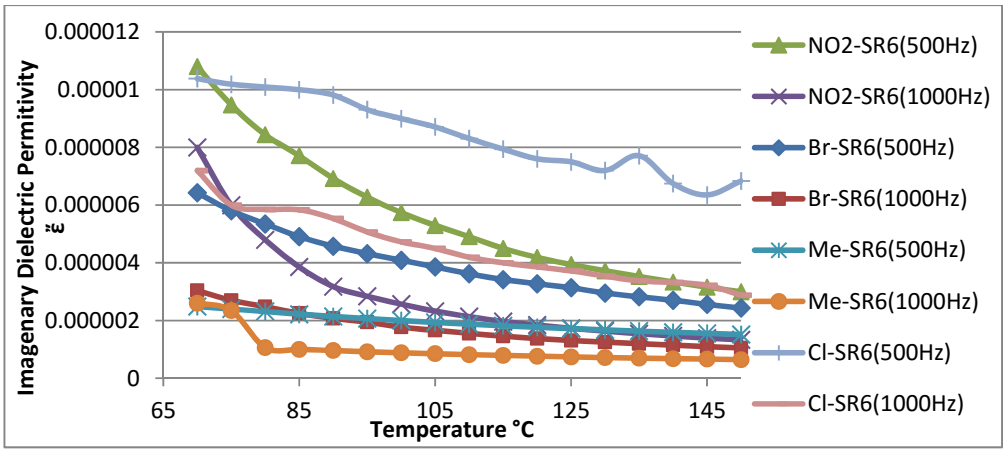

Figure (16) :Temperature dependence of imaginary dielectric permittivity at (500 and 1000) Hz for samples.

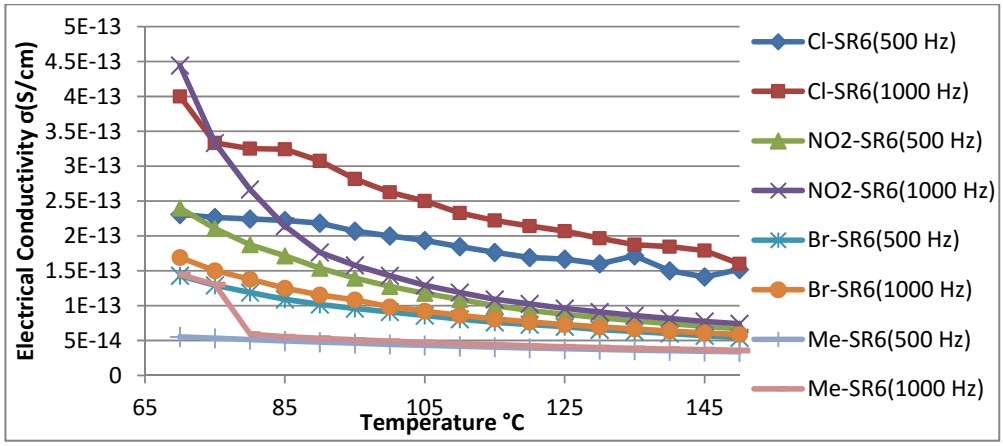

Figure (17):Temperature dependence of electrical conductivity at (500 and 1000) Hz for samples.

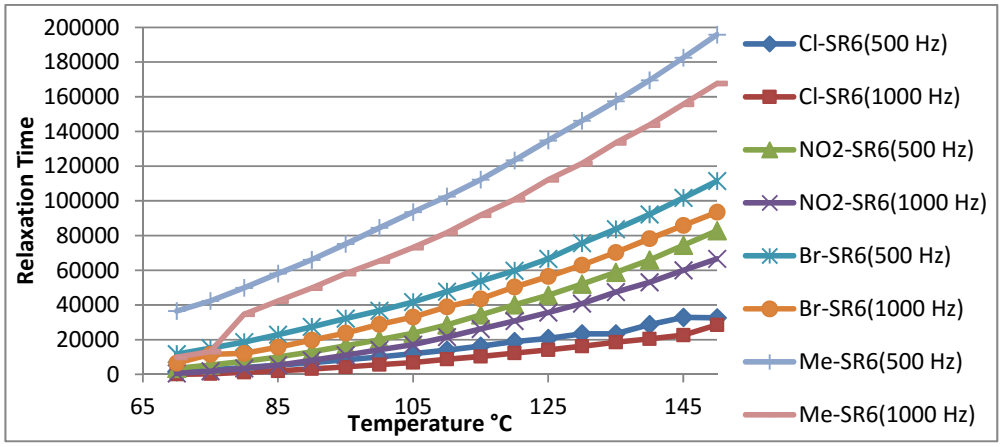

Figure (18): Temperature dependence of relaxation times at (500 and 1000) Hz for samples.

الخواص الميزومورفية والعزل الكهربائي لبلورات سائلة غير متجانسة الحلقة ذات مجاميع طرفية مختلفة

جمان أحمد ناصر
قسم الكيمياء/ كلية التربية للعلوم الصرفة (ابن الهيثم) / جامعة بغداد
استلم في:2016/2/22، قبل في:30/اذار/2016

الخلاصة

لقد تم تحضير أربع مركبات بلورية سائلة بمعوضات مختلفة بالموقع بارا (برومو، كلورو، نايترو، مثيل) وتم تشخيصها جميعاً بوساطة مطيافية الأشعة تحت الحمراء عالية الأداء FTIR ومطيافية الرنين النووي المغناطيسي ^{1}HNMR للمركبين [NO_2-SR_6] و[Cl-SR_6]. ثم درست الخواص البلورية السائلة لتلك المركبات باستعمال مجهر الضوء المستقطب والمزود بمنصة تسخين (POM)، كما تم تحديد انثالبيات و انتروبيات الانتقالات الطورية باستعمال مسعر المسح التفاضلي (DSC). وقد أظهرت جميع المركبات خواصاً ميزومورفية، إذ أبدى كل من المركبات [Br-SR_6] و [Cl-SR_6] و[NO_2-SR_6] . أطواراً سمكتية بالتسخين والتبريد بينما اظهر المركب [Me-SR_6] طوراً نيماتياً بالتبريد فقط. وعلى نحو متواصل درست خواص نفاذية العزل الكهربائي لتلك المركبات لمدى من الدرجات الحرارية (70-150)°م بترددين مختلفين هما 500 Hz و 1000 Hz. وبصورة عامة أبدت قيم كل من نفاذية العزل الكهربائي و زمن الاسترخاء زيادة مع زيادة درجة الحرارة، بينما أبدت قيم التوصيلية الكهربائية نقصاناً مع ازدياد درجات الحرارة. ثم تم حساب قيم طاقات التنشيط بيانياً باستعمال معادلة ارينيوس.

الكلمات المفتاحية: غير متجانس الحلقة، قواعد شف، نيماتي، سمكتي، بلورات سائلة، نفاذية العزل الكهربائي، توصيلية كهربائية، زمن استرخاء، طاقة تنشيط.